

THE USE OF AEROMAGNETIC DATA IN REGIONAL CRUSTAL STUDIES AT LOW LATITUDES: A CASE STUDY

M.S.M. MANTOVANI and W. SHUKOWSKY

*Instituto Astronômico e Geofísico — Universidade de São Paulo
Caixa Postal 30627 — 01051 — São Paulo — Brasil*

A large extent aeromagnetic survey (c.a. 10^6 km²) covering the states of Minas Gerais and Espírito Santo (DNPM, 1974) is used to illustrate and discuss the numerical methods required for the recovery of long wavelength anomalies which are usually suppressed by the processing normally applied to aeromagnetic data for exploration geophysics purposes.

The use of global primary field models as a reference was found to be adequate for the regional anomaly computation, even though these models are not the best representation of the primary field in the survey area.

It is also shown that the reduction to the pole, when applied to the survey has a good performance despite the non planarity of the reference surface, the low geomagnetic latitude and the large directional variation of the reference field in the survey area.

Um levantamento aeromagnético de grande extensão ($\sim 10^6$ km² — Minas Gerais e Espírito Santo — Brasil) foi utilizado para ilustrar e discutir métodos numéricos que permitem recuperar as anomalias de longo comprimento de onda que usualmente são suprimidos no processamento padrão usado na confecção de mapas de anomalia para fins de prospecção geofísica.

Verificou-se que a utilização de modelos globais do campo principal é adequada para o estudo das anomalias regionais, apesar destes modelos sabidamente não representarem bem o campo principal na região SE Brasileira.

Mostra-se também que a redução ao pólo, aplicada ao levantamento, apresenta bons resultados mesmo quando a anomalia é referida a uma superfície esférica, e nas condições de baixa inclinação geomagnética e de variações apreciáveis do campo de referência.

INTRODUCTION

During the last few years the long wavelength magnetic anomalies in continental areas have been intensively studied in order to determine the magnetic structure of the lithosphere.

The bottom of the magnetized layer has generally been considered as coincident with the Curie isotherm of pure magnetite (580°C) which can reach well below the Moho for the geothermal gradients observed in stable regions (Blackwell, 1971; Hyndmann et al., 1968; McGetchin and Silver, 1972; Rao and Jaeger, 1975). Haggerty (1976) and Gasparini et al. (1979) pointed out that it is probably not correct to assume a single Curie point for lower crustal rocks, being possible to have Curie temperatures lower than 300°C, depending on the composition and oxidation state of titanomagnetites, or higher than 580°C, if serpentinization processes occur. Wasilewsky et al. (1979) has shown that long wavelength magnetic anomalies cannot have sources in the mantle, based on magnetic measurements of some mantle derived rocks.

In a previous work (Mantovani and Shukowsky, 1982), a single aeromagnetic survey covering a large extent of the São Francisco craton (Almeida, 1977) was used to

determine the magnetic structure of the deep crust in a low heat flow area by spectral methods. Several numerical procedures designed for the recovery of long wavelength anomalies from aeromagnetic data and for the reduction to the pole at low geomagnetic inclination briefly outlined at the time, are now discussed in detail with the belief that the acquired experience could be used in future regional geophysical investigations under similar conditions.

EXPERIMENTAL DATA

The aeromagnetic survey covering the states of Minas Gerais and Espírito Santo (DNPM, 1974) was obtained from the Companhia de Pesquisa de Recursos Minerais (CPRM). It is a very detailed one and was carried out by the Prakla company under a Brazil-Germany scientific joint agreement.

The total intensity magnetic field was measured on profiles by Geometric proton magnetometers (G803) and recorded on magnetic tape at a sampling interval of one second, i.e. about every 700 m considering the average aircraft velocity. The total area was divided into regions of similar topography, to permit flights at a constant altitude of about 400 m above ground level (a.g.l.). A total of

2.10^5 linear kilometers were flown in E-W direction with 2 km spacing and check profiles directed N-S every 20 km. The readings were reduced to a standard altitude of 1.2 km above sea level (a.s.l.) considering a 2 nT/100 m theoretical vertical gradient.

The final results were presented in the form of 153 total intensity anomaly maps on the scale 1:100,000 in UTM projection, generally with 25 nT contour interval.

DATA REPRESENTATION AND CHOICE OF A REFERENCE FIELD MODEL

The anomaly maps derived from the aeromagnetic survey data are intended mainly for the use in exploration geophysics work, which is essentially of a local nature.

Since regional variations of the geomagnetic field do not bear information related to shallow anomaly sources, they are of no interest in this kind of application and it is a common practice to compute the anomaly maps by residuation of the total intensity data with respect to a regional model of the primary field, usually in the form of a low degree polynomial adjusted to the experimental data being residuated.

Conversely, for deep crustal studies the long wavelength anomalies are of crucial importance. To preserve them in the final anomaly it is required to residuate the total intensity survey data with respect to a global spherical harmonic model of the primary field.

In our case the original total intensity measurements, recorded on magnetic tape, were not available and had to be re-computed from the anomaly maps by adding back the regional field model initially subtracted. Because of the longitudinal extension of the survey, not only the anomaly maps but also the regional field model have been referred to two adjacent 6° UTM sectors with central meridians 45°W and 39°W for the western and eastern parts of the survey respectively.

The anomaly values were read from the maps at the nodes of a $5 \times 5 \text{ km}^2$ grid referred to the cartesian coordinates of the corresponding UTM sector. Then the total intensity values at the grid nodes were computed by adding to each of the 23,500 anomaly readings the value of the regional field given by

$$T(x,y) = 24,104.1 + 0.85914 x + 0.29025 y + 3.2743 \times 10^{-4} xy + 5.8690 \times 10^{-4} x^2 + 3.7519 \times 10^{-4} y^2 \quad (1)$$

$$x = X - 7,793.0$$

$$y = Y + 19.0$$

for the eastern part of the survey, and

$$T(x,y) = 24,104.1 + 0.85061 x + 0.31961 y + 3.2382 \times 10^{-4} xy + 6.0233 \times 10^{-4} x^2 + 3.6512 \times 10^{-4} y^2 \quad (2)$$

$$x = X - 7,800.0$$

$$y = Y - 610.0$$

for the western part of the survey.

The next step in the process of isolation of long wavelength anomalies was the re-computation of the recovered total intensity field values on an equiangular spherical grid because the original $5 \times 5 \text{ km}^2$ grids, while being regular inside each UTM sector, are discontinuous at the sector boundary, making it impossible to apply to the whole surveyed area any numerical procedure requiring a single regular data grid. The spherical re-gridding with a $0.1^\circ \times 0.1^\circ$ grid spacing was combined with a 0.1° low-pass filtering thus reducing considerably the size of the data set at the expense of the high frequency resolution, which is not important for regional studies.

The next problem to be solved was the choice of the best available primary field model to be used in the surveyed area. As our interest was directed to the long wavelength components of the anomalous field, it was not possible to use any model field computed directly from our data. On the other hand, Barraclough et al. (1978), showed that for many areas (especially near the magnetic equator) the secular variation from 1965 to 1975 predicted by the original IGRF model (Zmuda, 1971), was quite bad, becoming worse with the years elapsed since 1965.

Considering that the survey under analysis was carried out during 1971, it was not desirable to use the original IGRF 65 model.

An improved model (IGRFD) was calculated by Barraclough et al. (1978), including all data used for the original IGRF 65 model plus all secular variation data recorded during the 1965-1975 time interval. A comparison between the two IGRF models can be seen in Fig. 1 (a) and (b) where the differences between each of them and a second degree polynomial fit to our aeromagnetic survey data (2CM) is shown. A comparison between the two

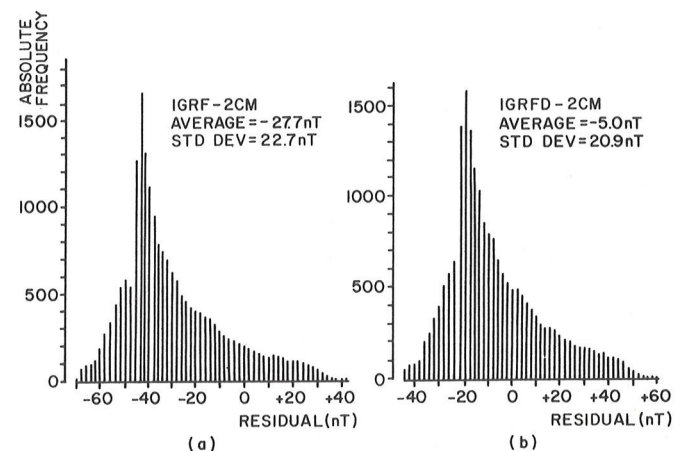


Figure 1 — Distribution of anomalous values of IGRFD (a) and of IGRF (b) when compared to the second degree surface (2CM) adjusted to the experimental data.

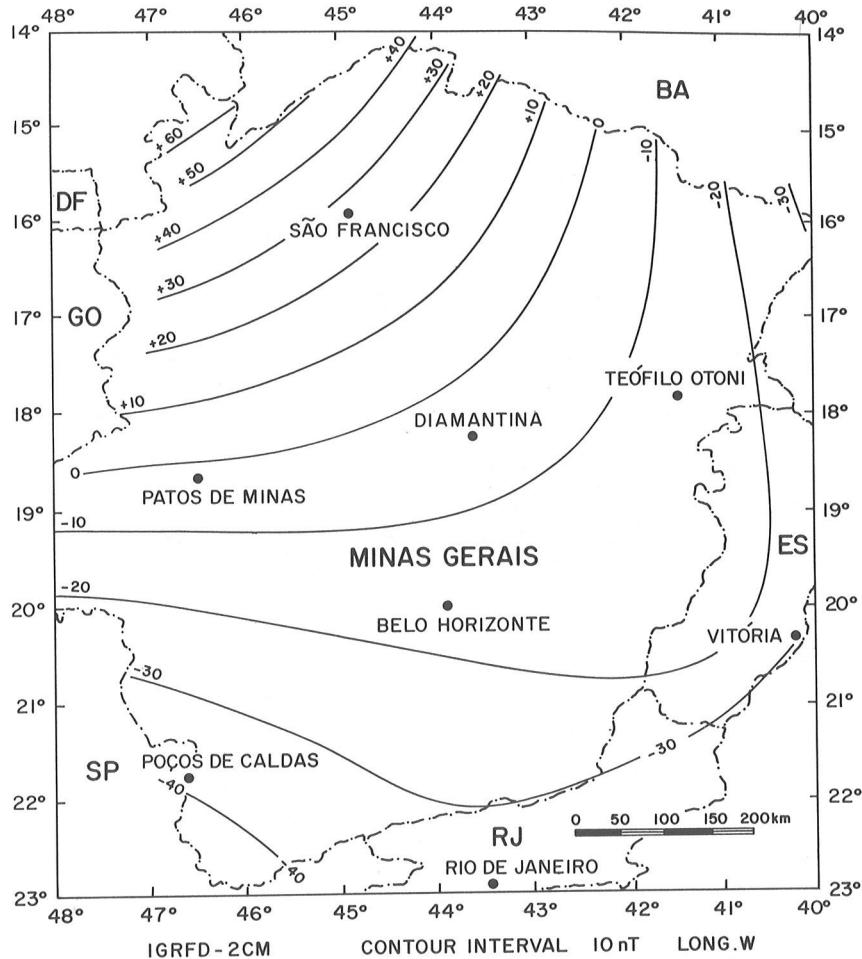


Figure 2 — IGRFD - 2CM residual field calculated for the entire area of survey. Contour interval is 10 nT.

histograms shows that the IGRFD model approximates better the second degree polynomial fitted to the data (Average (IGRF - 2 CM) = -27.7 nT and Average (IGRFD - 2CM) = -5.0 nT). The IGRFD model was therefore chosen as the reference field. However, it must be pointed out that while it is the best approximation to the real field available at present, it is by no means adequate to model the primary field in the surveyed area. This can be seen when the difference (IGRFD - 2CM) (Fig. 1b) is plotted on a map of the surveyed area (Fig. 2). A clear NW-ward trend can be observed with values increasing gradually from -30 nT at SE to +60 nT at NW. This trend seems to be part of an anomaly with a wavelength much longer than 1500 km, possibly in the resolution range of the field model. Fig. 3 shows a contour map of the total intensity anomaly computed with respect to the IGRFD model.

The anomalies shown in Fig. 3 can be grouped into three categories: the small size anomalies with $\lambda \leq 30$ km, the intermediate size anomalies with $30 \text{ km} < \lambda \leq 150$ km and the regional anomalies with $150 \text{ km} < \lambda$.

The small size anomalies are very numerous, but have been considerably attenuated by the low pass filtering at $\lambda = 0.1^\circ$. The intermediate size anomalies are

located approximately at (19°S, 47°W), (22°S, 46°W), (20°S, 43.5°W), (19°S, 42.5°W), (16°S, 41°W), (21°S, 41°W) and (17.5°S, 44.5°W), the latter showing a reversed polarization pattern. The regional anomalies form a series of broad ENE lineations with a wavelength around 300 km, an amplitude of 60 nT peak to peak, and are seemingly not related to the structural trends in the area oriented mainly in NNW and NS directions (Almeida, 1981).

REDUCTION TO THE POLE

In order to better correlate the anomaly pattern with the structural trends in the surveyed area as well as to apply spectral depth estimation techniques (Spector and Grant, 1970), the total intensity anomaly map of Figure 3 was reduced to the pole. The reduction was performed by assuming a fixed direction for the reference field with the inclination and declination equal to the values computed from IGRFD for the center of the surveyed area ($I = -21.00^\circ$, $D = -18.75^\circ$).

In order to satisfy the conditions required for the reduction to the pole (Baranov, 1975), the transformed

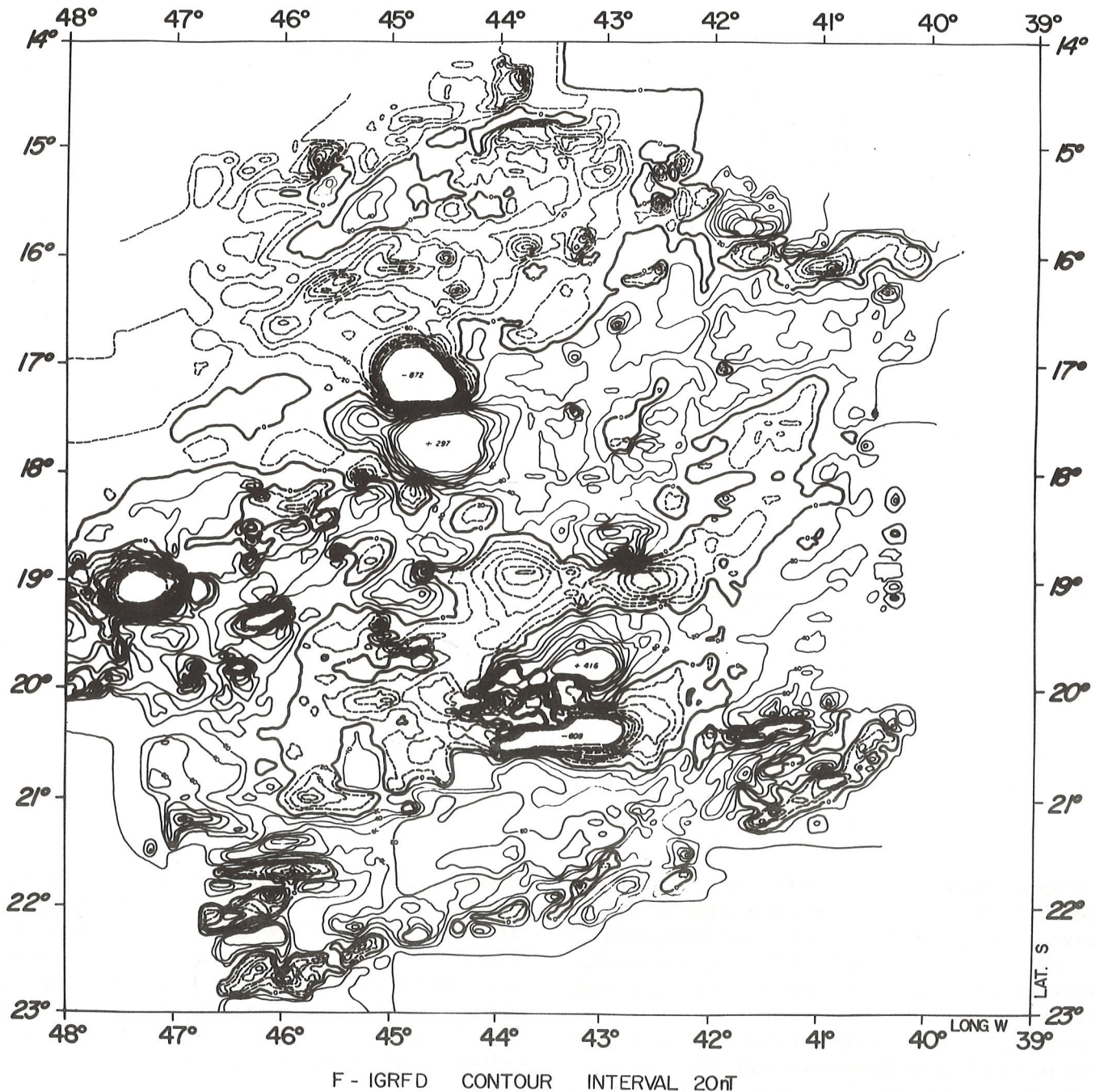


Figure 3 — Observed anomaly map referred to the IGRFD model constructed on a grid $0.1^\circ \times 0.1^\circ$. Contour interval is 20 nT.

anomaly field was carefully checked for the effects of neglecting the sphericity of the reference surface, the directional variation of the reference field in the area and of assuming a purely induced magnetization.

It was observed that all small and intermediate size localized anomalies, i.e. those exhibiting a clearly defined dipolar pattern behaved satisfactorily, showing a strong enhancement of the maximum relative to the minimum for normal anomalies, and of the minimum relative to the maximum for the reversed ones.

The regional anomalies in the form of ENE lineations, probably associated to deep seated sources of large lateral extent, have been transformed in a completely different manner to that of the local anomalies: in the reduced to the pole anomaly map the ENE lineations were replaced by lineations with a higher amplitude (c.a. 200 nT pp) elongated in a direction close to NNW. The situation can be observed in Figures 4 (a) and 4 (b) which show the original and the transformed anomaly maps respectively, represented in a form designed to enhance the visibility of long wavelength patterns.

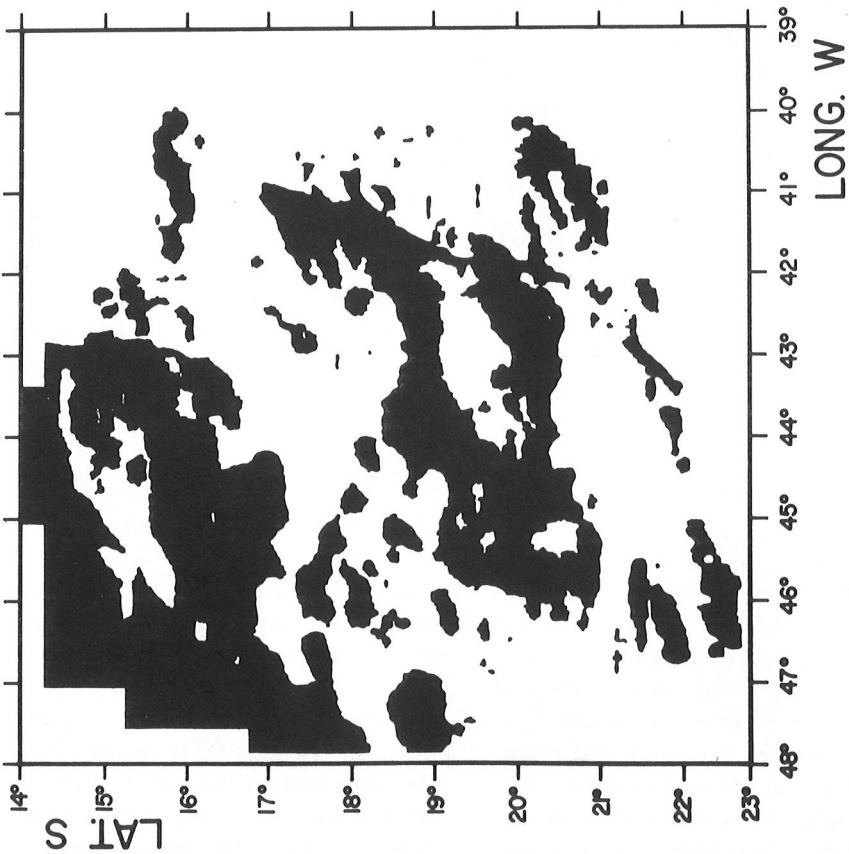


Figure 4a — Original long wavelength anomaly pattern.

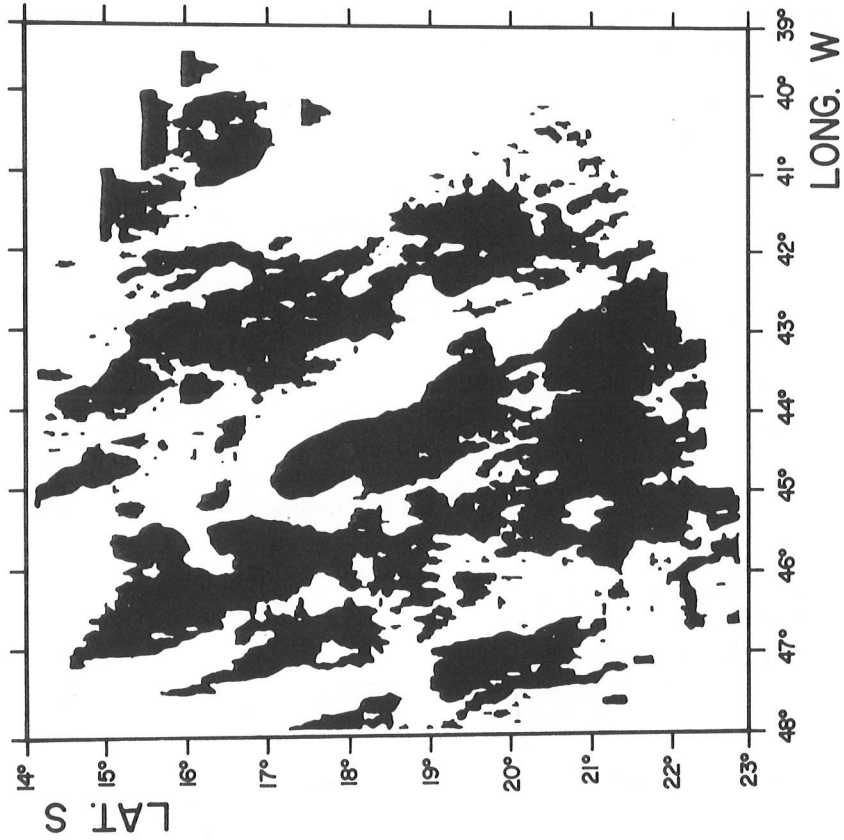


Figure 4b — Reduced to the pole long wavelength anomaly pattern. Shaded areas are negative.

By a closer examination of the reduction to the pole transform in the frequency domain it can be shown, that this apparently unusual behaviour of the regional anomaly is characteristic for low geomagnetic latitudes.

For the data sampled on a regular $(2M + 1) \times (2M + 1)$ grid, the total intensity anomaly can be represented by a complex bivariate trigonometric polynomial of degree M . (Battacharyya, 1965; Hahn, 1957):

$$T(x, y) = \sum_{n=-M}^{+M} \sum_{m=-M}^{+M} C_{n,m} \exp [2\pi i (u_n x + v_m y)] \quad (3)$$

$$0 \leq x \leq L, \quad 0 \leq y \leq L$$

which interpolates the sampled data on the grid points (x_k, y_j) defined by

$$x_p = y_p = L p / 2M, \quad p = 0, 1, 2, \dots, 2M. \quad (4)$$

The set of coefficients $C_{n,m}$ forms the discrete complex amplitude spectrum of the grid data usually computed by the FFT algorithm. The quantities u_n, v_m in eq. (3) are discrete values of the spatial frequency along the x and y axes respectively, defined by

$$u_k = v_k = k/L, \quad k = -M, -M + 1, \dots, +M.$$

L being the lateral extent of the surveyed area.

Because the anomaly is a real quantity, $C_{n,m}$ and $C_{-n,-m}$ are complex conjugates and therefore for each n, m (except $n=m=0$), the two terms corresponding to $C_{n,m}$ and $C_{-n,-m}$ add together into a real quantity.

If $C_{n,m} = a_{n,m} + i b_{n,m}$ then eq. (3) can be rewritten as

$$T(x, y) = \sum_{n=0}^M \sum_{m=-M}^M T_{n,m}(x, y) \quad (5)$$

$$\text{with } \begin{cases} T_{0,0}(x, y) = a_{0,0} \\ T_{n,m}(x, y) = 2 |C_{n,m}| \cos [2\pi (u_n x + v_m y) - \phi_{n,m}] \end{cases} \quad (6)$$

for all $n + |m| \neq 0$

$$\text{where } \phi_{n,m} = \tan^{-1} (b_{n,m}/a_{n,m}). \quad (7)$$

The functions $T_{n,m}$ will be called "partial anomaly waves". A closely related set of functions was defined by Hahn (1957) for the study of magnetic fields generated by the harmonic distribution of magnetization in the crust.

A partial anomaly wave $T_{n,m}$ is completely determined by the corresponding complex Fourier coefficient $C_{n,m}$ which characterizes its amplitude, frequency and phase. The frequency is a 2-vector quantity expressed either through its components along the x and y axes, u_n, v_m respectively, or through the radial frequency $S_{n,m}$ and azimuth $\theta_{n,m}$ defined as:

$$\begin{cases} S_{n,m} = \sqrt{u_n^2 + v_m^2} \\ \cos \theta_{n,m} = u_n / S_{n,m} \\ \sin \theta_{n,m} = v_m / S_{n,m} \end{cases} \quad (8)$$

The total intensity anomaly reduced to the pole is defined in analogy with eq. (3) by:

$$T'(x, y) = \sum_{n=-M}^{+M} \sum_{m=-M}^{+M} C'_{n,m} \exp [2\pi i (u_n x + v_m y)] \quad (9)$$

$$\text{where } C'_{n,m} = C_{n,m} R_{n,m}. \quad (10)$$

Let the constant directions of the reference and polarization fields be defined by the unit vectors \vec{f} and \vec{p} respectively. The operator $R_{n,m}$ for the reduction to the pole is then expressed as

$$R_{n,m} = \frac{S_{n,m}^2}{\{i (f_x u_n + f_y v_m) + f_z S_{n,m}\} \{i (p_x u_n + p_y v_m) + p_z S_{n,m}\}} \quad (11)$$

Let I_f, D_f be the inclination and declination of the reference field, and I_p, D_p those of the polarization. Then, expressing the frequency vector in polar coordinates and after some transformations, it follows that

$$R_{n,m} = \frac{1}{\{\sin I_f + i \cos I_f \cos (D_f - \theta_{n,m})\} \{\sin I_p + i \cos I_p \cos (D_p - \theta_{n,m})\}} \quad (12)$$

Let us furthermore assume that $I_f = I_p = I$ and $D_f = D_p = D$. This is a common assumption when no information regarding the remanent magnetization exists. Eq. (12) then takes the form

$$R_{n,m} = \frac{1}{\{\sin I + i \cos I \cos (D - \theta_{n,m})\}^2} \quad (13)$$

From eqs. (10) and (13) it follows that the transformation of the Fourier coefficients of the anomaly, and hence of the partial anomaly waves (6), depends only on the azimuth of the corresponding frequency vectors. Therefore for the anomaly waves running along the geomagnetic meridian ($\theta_{n,m} = D$) it results $|R_{n,m}| = 1$. In this case the reduction to the pole will involve a change of phase without a change of amplitude. Conversely, for the anomaly waves running orthogonally to the magnetic meridian, $R_{n,m} = 1/\sin^2 I$ is a real number and always greater than 1.

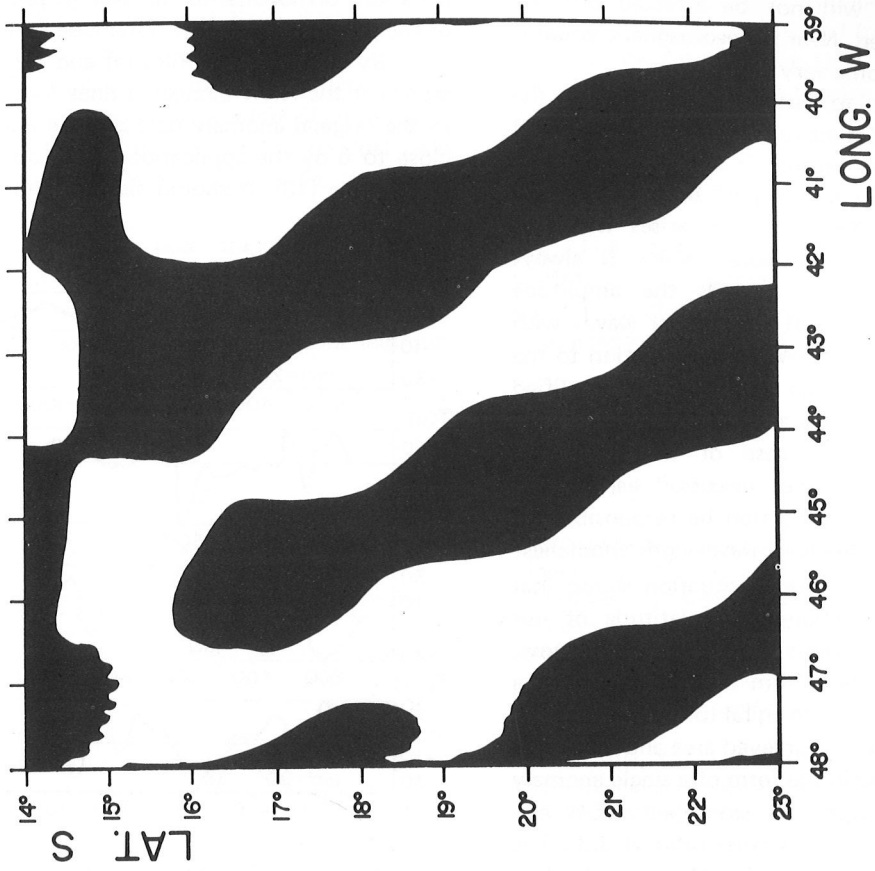


Figure 5b — The anomaly pattern in Fig. 5(a) reduced to the pole by the same operator as used in the surveyed area.

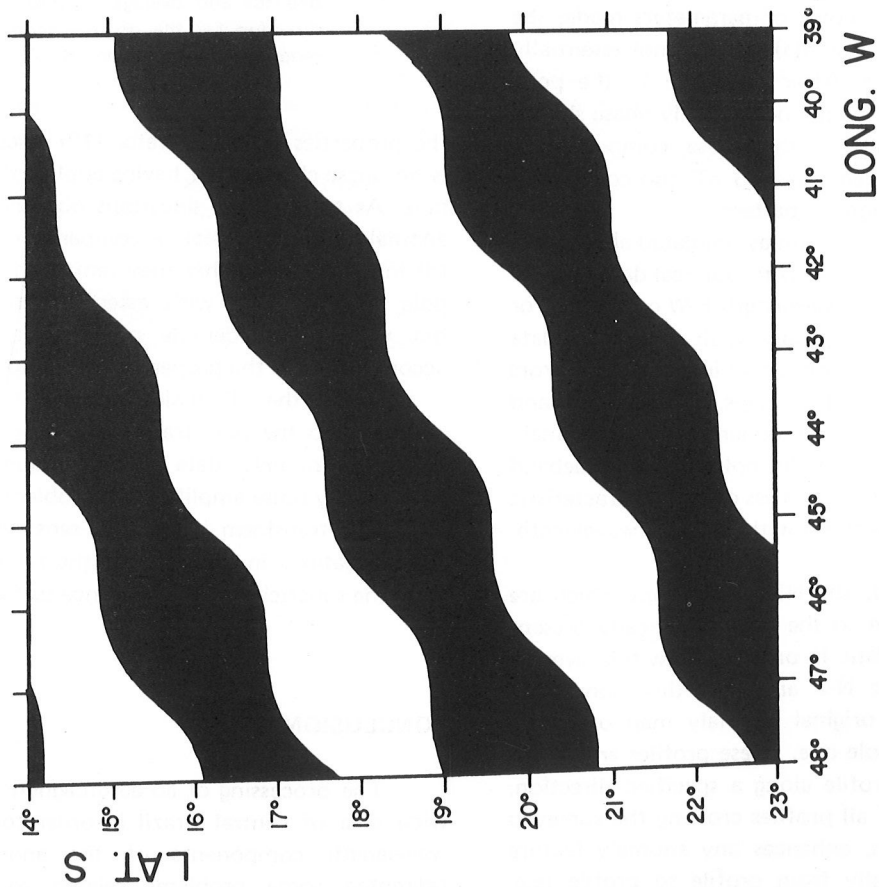


Figure 5a — Anomaly pattern produced by a single anomaly wave in magnetic N-S direction and amplitude of 100 nT affected by noise in magnetic E-W direction and amplitude of 30 nT. The wavelength of signal and noise is equal to 300 km..

In this case, the phase will not be affected but the amplitude will be magnified. Near the geomagnetic equator this magnification can become very large.

The effect of the azimuthal anisotropy of the operator (13) on the total intensity anomaly in the surveyed area was carefully verified because it can be a source of instability of the reduction to the pole transform at low geomagnetic inclinations. This situation arises whenever the amplitude spectrum of the noise, which is always present in experimental data, exceeds the amplitude spectrum of the anomaly signal for partial waves with azimuth close to geomagnetic E-W. After reduction to the pole these noise components can be so strongly amplified as to completely corrupt the final anomaly pattern.

Clearly this is not the case of the small and intermediate size local anomalies discussed earlier; but could the selective noise amplification be responsible for the observed behaviour of the long wavelength anomalies?

The simulation of an extreme situation shows that noise amplification at the geomagnetic latitude of our survey can be a source of serious error. Figure 5(a) shows the anomaly pattern resulting from a combination of a single anomaly wave with azimuth equal to the geomagnetic declination in the center of the surveyed area and amplitude of 100 nT pp with the noise in the form of a single anomaly wave with the azimuth equal to geomagnetic E-W and the amplitude of 30 nT (signal to noise ratio of 3.3). The wavelength of both signal and noise components is close to that of the regional lineations in Figs. 4(a) and 4(b).

With the particular choice of parameters made, the noise is certainly visible in Fig. 5(a) but does not essentially alter the anomaly pattern. After reduction to the pole, Fig. 5(b), while the signal component is only phase shifted with the unit amplification, the noise component is amplified to a value in excess of 230 nT and completely dominates the resultant anomaly pattern.

Even though such a situation as simulated above were possible, it is highly improbable with our real data because unless some systematic long wavelength E-W oriented error has been committed during the survey, all noise in the data resulting essentially from random visual interpolation errors during the digitization of the maps, is wideband and isotropic. Therefore the noise component, which is strongly amplified by the reduction to the pole, is also wideband and will affect all anomalies regardless of their characteristic wavelength, and not only those with the long wavelength, as observed.

On the other hand, the NNW lineations which are revealed by the reduction to the pole are already present in the original anomaly data. In order to show this, average profiles in the magnetic N-S and E-W directions were computed for both the original anomaly map of Fig. 3 and the reduced to the pole one. These profiles are shown in Fig. 6. An average profile along a specified direction, defined as the average of all profiles crossing the surveyed area along that direction, enhances any anomaly feature which recurs systematically from profile to profile (e.g.

lineations orthogonal to the average profile) at the expense of the attenuation of non-systematic features.

By comparing profiles (a) and (b) in Fig. 6 it can be seen that the NNW elongated lineations are already present in the original anomaly data and are amplified by a factor close to 6 by the application of the operator of reduction to the pole (13). It should also be noted that according to

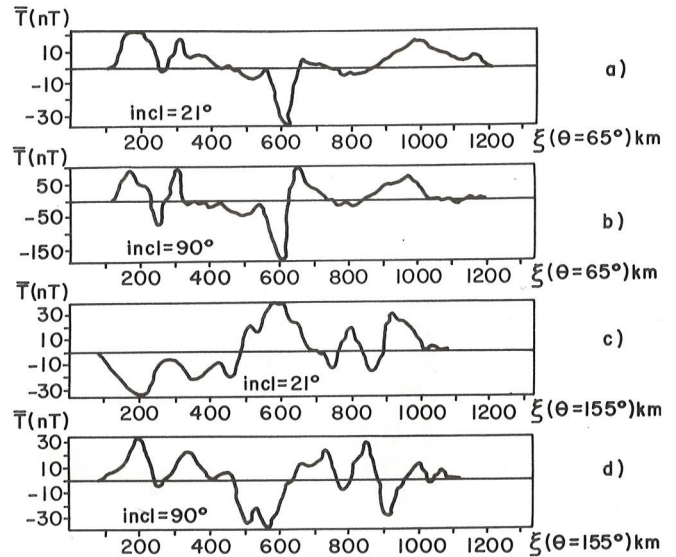


Figure 6 — Average profiles in the magnetic E-W direction for the original anomaly map (a) and the reduced to the pole one (b) and average profiles in the magnetic N-S direction for the original anomaly map (c) and the reduced to the pole one (d).

the properties of the operator (13) discussed earlier, there is no phase change after having applied the reduction to the pole. As to the ENE lineations observable in the original anomaly map, Fig. 4(a), a comparison of profiles (c) and (d) in Fig. 6 shows that they remain in the reduced to the pole anomaly map with essentially the same amplitude but with a considerable phase shift, which is also in accordance with the properties of the operator (13).

From the discussions above it follows that the reduction to the pole transform is applicable to the total intensity anomaly data at inclinations as low as 21° without any noise amplification problem.

The transform is also not sensitive to the relatively large variations in direction of the reference field, as well as to the sphericity of the reference surface.

CONCLUSIONS

The processing of an aeromagnetic survey covering a wide area of central Brazil in order to identify the long wavelength components of the anomalous field, has presented some problems related to the geographical

location of the survey. The first problem is the choice of an adequate model for the primary field. Although the IGRF model described by Barraclough et al. (1978) seems to be the best model available for the surveyed area at the time of the survey, the persistence of a NW-SE trend with a wavelength higher than 1500 km in the residual field indicates that the model does not account for the entire primary field.

The reduction to the pole transform, which is necessary in order to equalize the relative amplitudes of anomalies produced by bodies of different orientations, but has a reportedly poor performance at low inclinations,

has been shown to be applicable to anomaly data at inclinations as low as 21° and for a considerable change in direction of the reference field over the surveyed area, as well as for a non planar reference surface.

ACKNOWLEDGEMENTS

The referee's comments and suggestions have contributed to improve the first version of the manuscript and are gratefully acknowledged. This work was financially supported by CNPq and FINEP.

REFERENCES

- ALMEIDA, F.F.M. de — 1971 — O craton de São Francisco. *Rev. Bras. Geoc.*, **7**: 349-364.
- ALMEIDA, F.F.M. de — 1981 — Brazilian Structural Provinces: An Introduction. *Earth Sci. Rev.* **17**, 1-29.
- BARANOV, W. — 1975 — Potential Fields and their Transformations in Applied Geophysics. Gebrüder Bornträger — Berlin.
- BARRACLOUGH, D.R., HARWOOD, J.M., LEATON, B.R. and MALIN, S.R.C. — 1978 — A definitive model of the geomagnetic field and its secular variation for (1965). I. Derivation of model and comparison with the IGRF. *Geophys. J.R. astr. Soc.*, **55**: 111-121.
- BHATTACHARYYA, B.K. — 1965 — Two dimensional harmonic analysis as a tool for magnetic interpretation. *Geophysics*, **30**: 829-857.
- BLACKWELL, D.D. — 1971 — The thermal structure of the continental crust in the structure and physical properties of the Earth's crust. J.G. Heacock ed., AGU Mono, **14**: 169-184.
- DNPM — 1974 — Retrospectivas das atividades do convênio Geofísica Brasil-Alemanha e trabalhos do centro de Geofísica Aplicada. Report of Ministério das Minas e Energia (DNPM) — Brasília.
- GASPARINI, P., MANTOVANI, M.S.M., CORRADO, G., RAPOLLA, A. — 1979 — Depth of Curie temperature in continental shields: a compositional boundary? *Nature*, **278**: 845-846.
- HAGGERTY, S.E. — 1976 — Opaque mineral oxides in terrestrial igneous rocks. In: Oxidemminerals, D. Rumble III ed.
- HAHN, A. — 1957 — Two applications of Fourier's analysis of the interpretation of geomagnetic anomalies. *J. Geomag. Geoelectr.* **17**: 195-225.
- HYNDMAN, R.D., LAMBERT, J.B., HEIER, K.S., JAEGER, J.C. and RINGWOOD, A.E. — 1968 — Heat flow and surface radioactivity measurements. In the Precambrian shield of Western Australia. *Phys. Earth Plan. Inter.*, **1**: 129-135.
- MANTOVANI, M.S.M. and SHUKOWSKY, W. — 1982 — Analysis of a large extent aeromagnetic survey near the geomagnetic equator (Minas Gerais, Brasil). *Pure Appl. Geophys.*, **120**: 784-794.
- McGETCHIN, T.R. and SILVER, L.T. — 1972 — A crustal upper mantle model for the Colorado Plateau based on observations of crystalline rock fragments in the Moses Rock Dyke. *J. Geophys. Res.*, **77**: 7022-7037.
- RAO, R.V. and JAEGER, J.C. — 1975 — A comparison of the thermal characteristics of shields. *Can. J. Earth Sci.*, **12**: 347-360.
- SPECTOR, A. and GRANT, F.S. — 1970 — Statistical models for interpreting aeromagnetic data. *Geophysics*, **35**: 293-302.
- WASILEWSKI, P.J., THOMAS, H.H., MAYEN, M.A. — 1979 — The Moho as magnetic boundary. *Geophys. Res. Lett.*, **6**: 541-544.
- ZMUDA, A.J. — 1971 — World magnetic survey 1957-1969. IAGA Bulletin n° 28. IUGG Publication, 206 pp.

Versão original recebida em Nov./82;
Versão final, em Set./83.